

Speckle-based holographic detection for non-contact Photoacoustic Tomography

C. Buj^{1,3}, J. Horstmann², M. Münter¹ and R. Brinkmann^{1,2}

¹Institute of Biomedical Optics, Universität zu Lübeck, Lübeck, Germany

²Medical Laser Center Lübeck GmbH, Lübeck, Germany

³Graduate School for Computing in Medicine and Life Sciences, Universität zu Lübeck, Lübeck, Germany

Abstract

The main problems of most state-of-the-art Photoacoustic Imaging approaches are long acquisition times and the requirement of acoustic contact. We introduce a very fast innovative holographic-optical full field non-contact detection method to overcome these problems. In order to increase the acquisition speed significantly, the surface displacements of the object, caused by the photoacoustic pressure waves, are interferometrically measured by a high speed camera in two dimensions. Phase alterations in the observed speckle field determined by Electronic Speckle Pattern Interferometry (ESPI) are used to identify changes in the object's topography. The total acquisition time can be reduced to 100 ms.

This approach was validated with a silicone phantom with an embedded spherical absorber. After recording the topography of the object over time, a tomographic reconstruction leads to the three dimensional location of the different absorbers. A reliable reconstruction proves the ability of the method.

1 Introduction

To overcome the depth resolution limitations of many optical imaging techniques like Optical Coherence Tomography OCT, Photoacoustic Imaging has become very popular in recent years. Photoacoustic Imaging is based on the emission of thermoelastic pressure waves, generated by absorbers subsequent to short-pulsed optical excitation (Fig. 1). The high optical contrast is caused by the chromophore-dependent absorption coefficient of the tissue. Thus, the choice of the correct wavelength, where the target structure has a high absorption coefficient and the surrounding tissue a lower, is crucial.

After the pulsed light has reached the tissue surface, it is distributed depending on scattering and absorption. Due to absorption by desired absorbing structure, its temperature

1. Pulsed irradiation



2. Light distribution inside the tissue



3. Absorption



4. Thermoelastic expansion



5. Propagation of Pressure transients



6. Signal detection

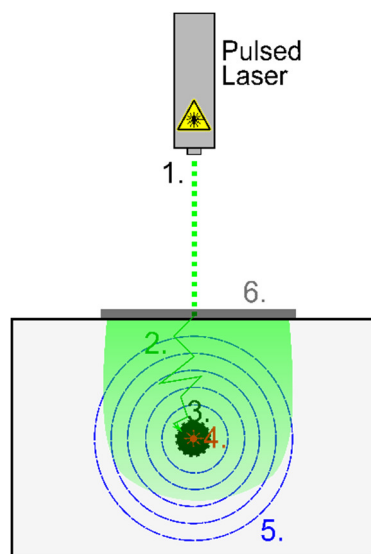


Fig. 1 Abstract schematic illustration of the photoacoustic effect, which is been used in different imaging techniques.

increases followed by a rapidly rising pressure. Thus, the absorber expands thermoelastically and pressure transients are emitted. Because of their low refraction and scattering, pressure waves can propagate large distances in tissue. In comparison to optical imaging techniques, this is a major advantage.

There are various methods to detect these pressure transients at the tissue surface. In many experimental setups, single element sensors are used. However, their use requires acoustic contact, and due to the need for mechanical scanning over the object a long acquisition time up to several minutes [1]. In particular for in vivo measurement, this is not acceptable because e.g. motion artifacts cannot be compensated.

For this reason, a novel holographic detection method that reduces the data acquisition time to 100 ms was developed. The main difference compared to classical piezoelectric detection is that surface displacements are measured in order to reconstruct the absorbing structures.

For tomographic imaging, the position of the absorbers can be reconstructed in three dimensions by post-processing the detected signals, using e.g. time reversal approaches like k-wave [2] or triangulation based algorithms like delay and sum [3].

2 Material and Methods

Fig.2 illustrates the principle of a novel holographic detection method. The detection laser light is scattered mainly in the superficial tissue. A Mach-Zehnder interferometer is the main component to measure the displacement of the tissue surface. The light of a reference wave interferes with the multiple backscattered object light which leads to a holographic interferogram that is detected by the high-speed camera. The individual components of the setup are controlled in a triple-pulse mode (Fig. 3).

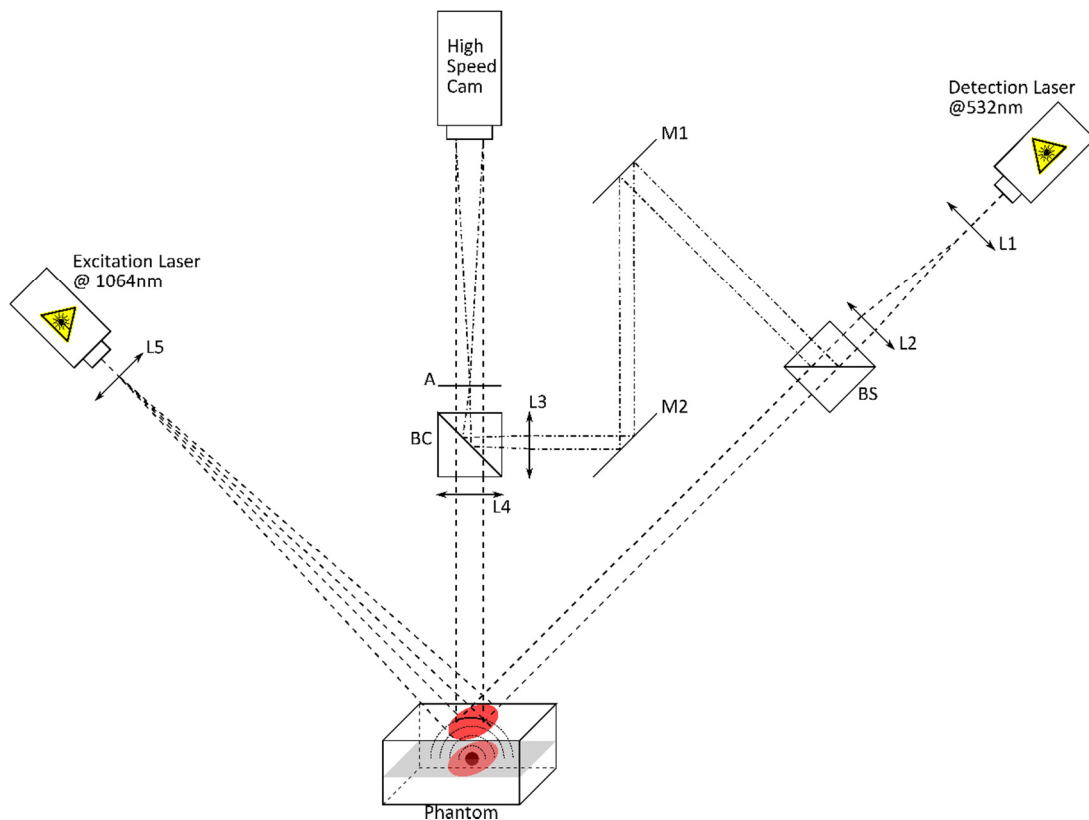


Fig. 2 Principle of the holographic-optical full-field measurement technique to determine the surface displacement. Main components of the system are a short pulsed excitation laser and a Mach-Zehnder interferometer that is composed of a short-pulse detection laser, a high-speed camera and optical components. After the excitation by the excitation laser, pressure waves are emitted by absorbers. With a defined delay thereon follows the illumination of the surface by the detection laser. The light of a reference wave interferes with the multiple backscattered object light which leads to a holographic interferogram that is detected by the high-speed camera.

In the first step, the phase distribution is measured. This measurement is used as a reference and makes the method insensitive to thermal expansions of the entire tissue due to the previous pulses, artefacts by viscoelastic attenuation of the free boundary or other motion artefacts. In the second step, the tissue is laminary irradiated with the excitation laser, resulting in generation of thermoelastic pressure waves by the absorber. In the third step, the altered phase distribution is determined after a time delay Δt relative to the excitation pulse. By subtracting the two phase distributions, the geometrical object surface displacement can be evaluated. In a repetitive measurement, the time delay is increased continuously by choosing appropriate trigger frequencies for the excitation and the detection laser.

The computed phase difference images contain the actual topographical displacements of the considered period, which are used for the reconstruction.

Based on the acquired surface displacements over time, the positions of the absorbers within the tissue can be tomographic reconstructed.

2.1 Proof of concept

To demonstrate the applicability of the detection approach, an experimental setup was created (Fig. 4). In this setup, a transparent silicone cube (Wacker Silicones RT604 A/B) of 10 mm edge length serves as tissue model. A highly absorbing black silicone spherical absorber of about 2 mm diameter is located inside the silicone cube.

One side of the cube is irradiated by a Nd:YAG laser (Quantel YG571C, wavelength 1064 nm, pulse duration 6 ns, pulse energy 25 mJ, spot size 5 mm, repetition rate 10 Hz). For the used excitation wavelength, the absorption coefficient of the black silicone was measured to be 29.6 cm^{-1} . The acoustic properties of the phantom material were measured to be $0.93 \text{ mm}/\mu\text{s}$ for the speed of sound and $0.62 \text{ kN}/\text{mm}^2$ for the elasticity modulus. The density is $0.79 \text{ g}/\text{cm}^3$. The thermal expansion coefficient is $2 \times 10^{-4} \text{ K}^{-1}$.

For ease of operation, the detection was performed on an orthogonal side of the phantom. To increase backscattering

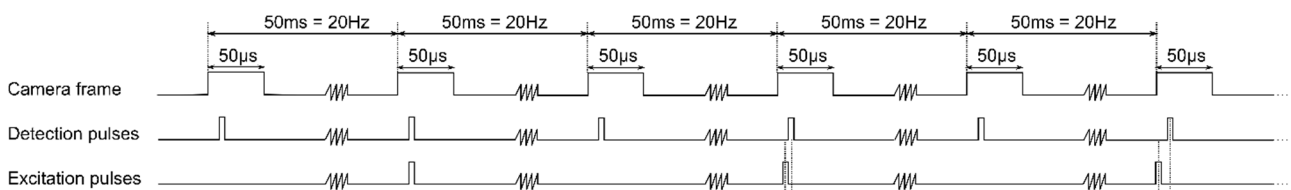


Fig. 3 Principle of the repetitive triple pulse detection mode.

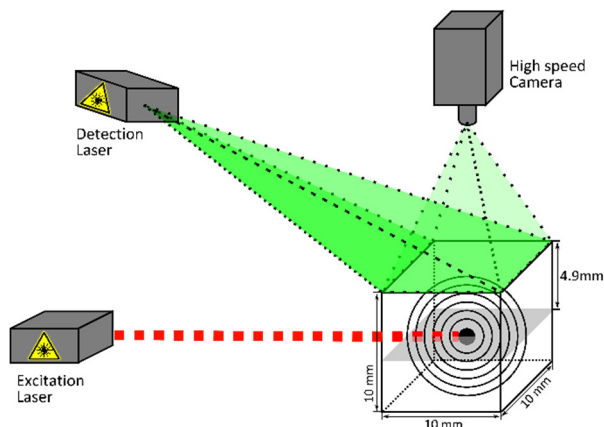


Fig. 4 Schematic illustration of the measurement of a spherical point absorber which has been positioned in a transparent silicone volume of 10 x 10 x 10 mm. The highly absorbing black silicone absorber has a diameter of 2 mm and was excited by a short pulsed laser.

of the detection laser light (CryLas FTSS 355-50, wavelength 532 nm, pulse duration 1 ns), the illuminated surface was coated with a 150 μm thick layer of white silicone. A CCD camera (Basler Pilot piA1600-35g, resolution 1600x1200 pixels, pixel size 7.4 μm) with a frame rate of 20 Hz was used to record the images. The temporal resolution of the measurement technique is about 100 ns.

The phase variations can be evaluated by Electronic Speckle Pattern Interferometry (ESPI) [4]. ESPI in Spatial Phase Shifting (SPS) Mode [5] is implemented, in order to get the phase information in a single image acquisition. In this approach, the lateral resolution of the phase measurement is influenced by the mean speckle size (4 pixels), the SPS phase period on the camera chip (4 pixels), the pixel pitch (7.4 μm) and the imaging scale (1).

In order to reduce speckle artefacts, a Gaussian blur filter with 12 pixels in size was applied to the complex phase maps. Validation measurements have shown that these parameters lead to a lateral resolution of 100 μm . The interferometric stability is restricting the axial resolution. For the presented setup it is about 4 nm.

The first tomographic reconstructions were performed in two dimensional space and have been carried out using the delay and sum algorithm as introduced by Carp and Venugopalan [6], which is similar to the Synthetic Aperture Focusing Technique (SAFT) [7].

As a reference measurement in order to determine the depth of the spherical absorber, the phantom was imaged with an SLR (Canon EOS 500D - 15.1 Megapixel CMOS-Sensor, Canon EF-S Objective 18-55mm). In the background of the phantom a graph paper was placed as scale.

3 Results and Discussion

3.1 Holographic measured surface displacements over time

In the presented measurement, 228 surface displacements were recorded, which lead after pre-processing to 114 temporally phase difference images. A small representative selection of these can be seen in Fig. 6. After 4.8 μs , a spherical displacement as an interaction of the spherical pressure

wave with the free boundary is visible. Assuming a sound velocity of 0.93 mm/ μs , we expect a depth position of the surface of the absorber of 4.46 mm. In the further course, the circular displacement spreads omnidirectional and is reflected at the boundary surfaces of the phantom. Due to existing hardware limitations the measurement is not equidistant in time.

3.2 Photographic specified position of the spherical absorber

Fig. 5 shows the result of the photographic determination of the distance between the phantom surface and the absorber. With the knowledge of the pixel pitch, the distance between the phantom surface and the surface of the absorber can be determined to be 3.95 mm. Because the absorber has a measured diameter of 1.95 mm, its center is located at a depth of approximately 4.9 mm. Due to many possible aberrations of this measurement method, these results serve only as approximate reference values. Nevertheless, this depth value differs only slightly from the depth value, which has been estimated based on the displacement measurements. In theory, a surface displacement should become visible after 4.2 μs . Because of the current measurement sensitivity, this small displacements are not detectable.

In prospective phantom measurements, the depth of the absorber should be determined by OCT, which will increase the accuracy of the reference method.

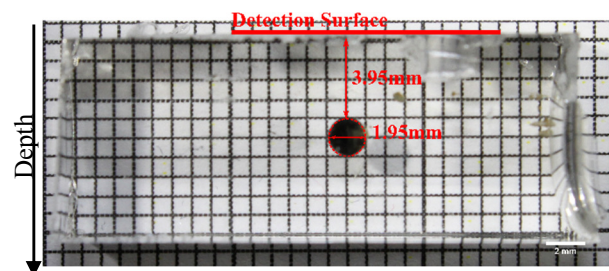


Fig. 5 Results of the photographic localization: Distance between the spherical absorber and the surface of the phantom is 3.95 mm. The center of the absorber is located at a depth of 4.9 mm.

3.3 Reconstructed position of the spherical absorber

For the two-dimensional reconstruction, a line was extracted from the surface displacement data set, which crosses the epicenter of deformation. The result after performing a threshold filter is shown in Fig. 7. Accordingly, the center of the absorber is at a depth of 4.9 mm.

Crucial for the validity of the edge structures is the choice of the threshold value, which was executed for artefact and noise suppression. This has the disadvantage that the information of the contours of the absorber are also extinguished.

In further studies, the reconstruction algorithm should be validated in terms of its accuracy with respect to the absorber geometry. Moreover, the number of the absorbers in the phantom, and a varying configuration should be analyzed.

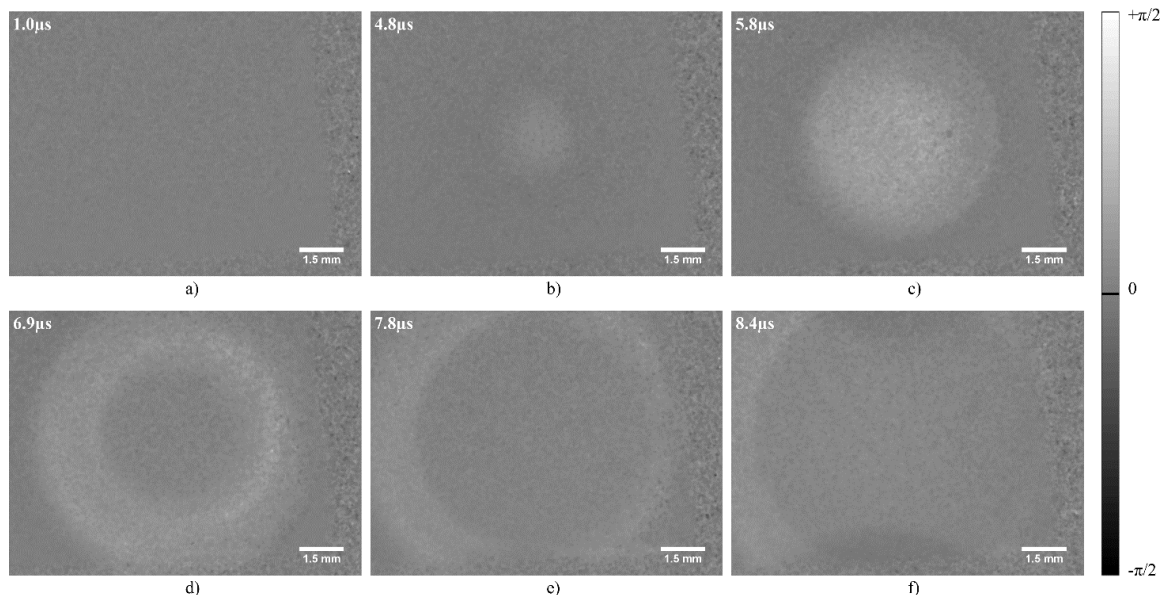


Fig. 6 Surfaces displacements at different times. a) $1.0\mu\text{s}$: Flat surface - pressure waves are still on their way b) $4.8\mu\text{s}$: A centered circular displacement becomes visible. c) $5.8\mu\text{s}$: The circular displacement increases omnidirectional. d) $6.9\mu\text{s}$: An annular wave was formed. e) $7.8\mu\text{s}$: Annular wave has spread. f) $8.4\mu\text{s}$: Annular wave has spread and was reflected at the boundary surfaces of the phantom.

In addition, the algorithm will be expanded to reconstruct the contours.

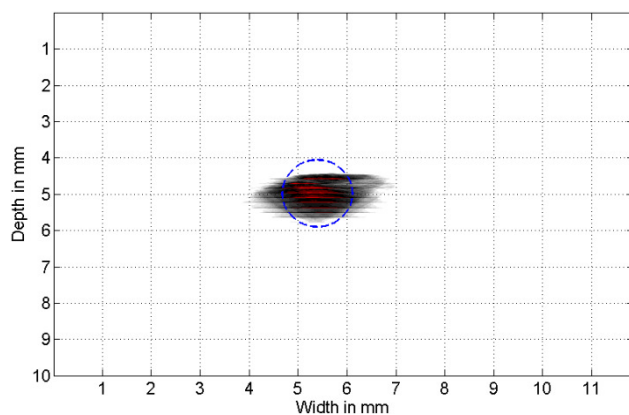


Fig. 7 Results of the reconstruction algorithm after performing a threshold filter. Depth of the center: 4.9 mm

4 Conclusions and outlook

With the results presented in this paper it could be shown that non-contact displacement measurement is a suitable approach for photoacoustic detection. In addition, the reconstructed positions agree well with the values determined by a reference measurement method. In the following steps, the sensitivity will be increased. For comparison with other detection methods the noise equivalent pressure (NEP) value should be determined.

5 Acknowledgements

This publication is a result of the ongoing research within the LUMEN research group, which is funded by the German Federal Ministry of Education and Research (BMBF, FKZ 13EZ1140A/B). LUMEN is a joint research project

of Lübeck University of Applied Sciences and Universität zu Lübeck and represents an own branch of the Graduate School for Computing in Medicine and Life Sciences of Universität zu Lübeck.

6 References

- [1] Xu M., L. Wang V.: Photoacoustic imaging in biomedicine. *Review of Scientific Instruments*, vol. 77, no. 4, (2006).
- [2] Treeby, B., Cox, B.: k-Wave: MATLAB toolbox for the simulation and reconstruction of photoacoustic wave fields. *Journal of Biomedical Optics*, 15(2), 021314 (2010).
- [3] Hoelen, C., de Mul, F.: Image reconstruction for photoacoustic scanning of tissue structures. *Applied Optics*, 39, 5872-5883 (2000).
- [4] Pedrini, G., Pfister, B., Tiziani, H.: Double pulse-electronic speckle pattern Interferometry. *Journal of Modern Optics*, 40 (1), 89-96 (1993).
- [5] Helmers H., Burke J.: Performance of spatial vs. temporal phase shifting in ESPI. *Proc. SPIE 3744*, 188-199 (1999).
- [6] Carp S., Venugopalan V.: Optoacoustic imaging based on the interferometric measurement of surface displacement. *Journal of Biomedical Optics*, 12(6), 064001 (2007).
- [7] Feng, D., Xu, Y., Ku, G., Wang, L.V.: Microwave-induced thermoacoustic tomography: Reconstruction by synthetic aperture. *Medical physics* 28, 2427-2431, (2001).
- [8] Horstmann, J., Brinkmann, R.: Optical full-field holographic detection system for non-contact photoacoustic tomography. *Proc. SPIE 8943-55* (2014).